Research Square

Preprints are preliminary reports that have not undergone peer review.
They should not be considered conclusive, used to inform clinical practice,
or referenced by the media as validated information.

The Exploration of Metabolic Biomarkers blood Lipidomics and Proteomics for diagnosing Alzheimer's disease

Shouzi Zhang

lanczsz@126.com

Beijing Geriatric Hospital

Tinyu Zhao

Beijing Geriatric Hospital

Yin Yuxin

yinyuxin@bjmu.edu.cn

Peking University

Ting Wang

Children's Medical Center of Peking University First Hospital, Beijing

Zihui Sun

Zhejiang Provincial Clinical Research Center for Mental Disorders, School of Mental Health, Wenzhou Medical University

---

Research Article

Keywords: Alzheimer's disease, amino acid, lipidomics, metabolic biomarker, proteomics

Posted Date: February 27th, 2026

DOI: https://doi.org/10.21203/rs.3.rs-8972322/v1

License: This work is licensed under a Creative Commons Attribution 4.0 International License.
Read Full License

Additional Declarations: The authors declare no competing interests.

Abstract

Introduction

Alzheimer's disease (AD) is the most common neurodegenerative disorder; however, its underlying mechanisms remain incompletely understood, posing challenges for early diagnosis. This study aimed to explore potential metabolic biomarkers for AD in blood.

Methods

We recruited 82 participants, including 47 AD patients (age: 80.2 ± 0.9 years) and 35 healthy controls (age: 77.6 ± 1.7 years). Blood samples were collected and analyzed using liquid chromatography-tandem mass spectrometry (LC-MS/MS) and high-performance liquid chromatography coupled with Q-Exactive HF MS. Data processing was performed using MS-DIAL, Skyline, and MaxQuant software. Metabolic pathway analysis was conducted with MetaboAnalyst, and enrichment analysis of differential metabolites was based on the KEGG database.

Results

Significant alterations were observed in amino acid metabolic pathways, including lysine degradation, pyruvate metabolism, glycine, serine and threonine metabolism, linolenic acid metabolism, and arginine and proline metabolism. Lipidomics analysis revealed seven lipids that were significantly elevated in the AD group: Cer 40:9;O3, DG 25:0, DG 46:7, NAE 16:1, PC 20:1/22:5, PC O-35:5, and TG 45:7. Notably, receiver operating characteristic (ROC) curve analysis showed that the area under the curve (AUC) values for these seven lipids all exceeded 0.8.

Discussion

This comprehensive multi-omics approach effectively identified dysregulated plasma molecules in AD patients, suggesting that specific blood lipids may serve as potential biomarkers for AD diagnosis.

INTRODUCTION

Early screening and diagnosis have become increasingly important with the rising incidence of Alzheimer’s disease (AD). Amyloid-beta (Aβ) and phosphorylated tau protein are two core biomarkers of AD (Karran et al., 2011). Currently, cerebrospinal fuid (CSF) biomarkers and amyloid positron emission tomography (PET) imaging are not widely applied in clinical practice due to their invasiveness, limited accessibility, and high costs. Compared with CSF or PET examinations, plasma biomarkers are less invasive, more costeffective,and easier to implement. However, accurately quantifying Aβ in blood remains challenging due to its low concentration (Verberk et al., 2018). However, with the continuous improvement of detection technology, plasma biomarker detection has become the mainstream direction for AD diagnosis in the future.Food and Drug Administration (FDA) approved the first in vitro diagnostic device, the Lumipulse G pTau217/β-Amyloid 1–42 Plasma Ratio, for clinical use to aid in the

diagnosis of AD (Food and Drug Administration,2025). Metabolomics, which studies the complete set of metabolites within cells at a specific time point, reflects the cellular microenvironment (Ong and Mann, 2005; Wishart, 2016). With the rapid advancement of liquid chromatography-mass spectrometry (LC-MS)-based omics technologies (Wishart, 2016), it is now feasible to reliably analyze hundreds to thousands of metabolites from biological samples, providing valuable insights for biomarker discovery as well as pathological and biological research (Saito and Matsuda, 2010; Cravatt et al., 2007). Consistent with this, several metabolites have been found to be dysregulated in the blood of AD patients (Mahajan et al., 2020), suggesting their potential utility as diagnostic markers for AD (Sun et al., 2022).The combination of plasma metabolomic biomarkers with plasma Aβ biomarkers may enable more accurate early diagnosis of AD.We plan to conduct a plasma metabolomics study comparing Alzheimer's disease patients with elderly cognitively normal controls, with the aim of discovering potential biomarkers for early diagnosis and treatment of AD.

METHODS

Participants

Data were collected between January and May 2024 from a geriatric hospital and a nursing community . The cohort included cognitively normal controls (n = 35; mean age = 77.57±1.65 years) and patients with clinically diagnosed AD (n = 47; mean age = 80.15±0.94 years). AD diagnosis was made based on recommendations from the National Institute on Aging-Alzheimer’s Association workgroups on diagnostic guidelines for Alzheimer’s disease (McKhann et al.,2011).

Ethical statement

This study was approved by the Clinical Ethics Committee of Beijing Geriatric Hospital (Ethical Approval Number: BJLLYY-2024-009), in compliance with the principles of the Helsinki Declaration. Samples were collected only from patients who agreed to undergo this examination for laboratory research. The informed consent of blood donors was obtained, and all methods were conducted according to relevant guidelines and regulations.

Metabolomics sample processing

After fasting overnight, collect 4 mL of venous blood from the forearm circulation and transfer it to an EDTA-K2 vacuum tube. Centrifuge at 3000 x g for 20 minutes to separate the plasma, then store at-80 °C until analysis. Use liquid-liquid extraction to extract metabolites and lipids from the plasma sample as follows: extract 100 μL of plasma with four times its volume of cold chloroform: methanol (2:1). Vortex the mixture and centrifuge at 13,000 x g for 15 minutes. Collect the upper aqueous phase (hydrophilic metabolites) and the lower organic phase (hydrophobic metabolites), and vacuum evaporate under room temperature. Store the evaporated samples at-80 °C until LC-MS/MS analysis.

HPLC and Q-Exactive HF MS for metabolomics

Metabolomics and lipidomics were performed on the Ultimate 3000 ultra-high-performance liquid chromatography system and Q-Exactive HF MS (Thermo Scientific). The aqueous phase (metabolomics) was separated using a X bridge amide column (100 × 2.1 mm i.d.,3.5 μm; Waters), under 30 °C. Compounds were separated under 30 °C. Mobile phase A consists of a 5 mM ammonium acetate aqueous solution, and mobile phase B is acetonitrile. Flow rate is 0.4 mL/min, with a linear gradient as follows: 0 minutes, 95% B; 3 minutes, 90% B; 13 minutes, 50% B;14 minutes, 50% B; 15 minutes, 95% B; 17 minutes, 95% B. Samples were suspended in a 100 μL acetonitrile: water (1:1, v/v) solution, with an injection volume of 10 μL. Injection volume is 10 μL. Chromatographic separation of lipids was performed using an inverse-phase X-select CSH C18 column (2.1 mm × 100 mm, 2.5 μm, Waters Corporation) at a separation temperature of 40 °C.A binary solvent system was used (containing 10 mM ammonium acetate and 0.1% formic acid) for the gradient. Elution: (A) ACN/water (3:2, V/V), (B) IPA/ACN (9:1, V/V). The gradient procedure is as follows: 0 minutes-40% B; 2 minutes-43% B; 12 minutes-60% B; 12.1-75% B; 18 minutes-99% B; 19 minutes-set the flow rate to 0.4 ml/min. The sample is suspended in a 100 μL chloroform: methanol (1:1, v/v) solution and then diluted three times with isopropanol. It is further diluted three times with an isopropanol: acetone: H_2O (2:1:1, v/v/v) solution. The injection volume is 10 microliters.

Mass spectrometry for metabolomics

Mass spectrometry techniques used for metabolomics are based on data-dependent acquisition (DDA) and parallel reaction monitoring (PRM) Using Q-Exactive HF MS (Thermo Scientific). For DDA-MS, acquisition is performed separately in positive and negative ion modes. Each acquisition cycle includes one (MS1 scan) with a resolution of 60,000, covering the mass range of hydrophilic metabolites from 60 to 900 m/z, followed by 10 MS/MS scans in HCD mode. Ten MS/MS scans are performed at 30,000 resolutions. For PRM-MS, the m/z values for 14 target lipids (13 target lipids and 1 internal standard) are set in the inclusion list, with each acquisition cycle including one full MS1 scan at a resolution of 60,000 (from 200 m/z to 1200 m/z) and 14 MS2 scans targeting the specified lipid at 30,000 resolutions.

For DDA-MS and PRM-MS, the automatic gain control (AGC) target values are both set to 5e6 (maximum injection time 30 ms) and 2e5 (maximum injection time 100 ms). MS1 and MS/MS scans. Ion source parameters: spray voltage of 3.3 kV in positive ion mode, and 3.0 kV in negative ion mode. Spray voltage of 3.3 kV in positive ion mode, and 3.0 kV in negative ion mode; ion source sheath gas 40; auxiliary gas 10; capillary temperature 320℃; probe heater temperature 300℃; S-lens RF level 55. Samples (a total of 100) are analyzed in random order. Quality control (QC) samples: all research samples are mixed equally and analyzed every 10 samples throughout the chromatographic analysis process. Throughout the liquid chromatography-mass spectrometry analysis, one analysis is performed every 10 samples.

DDA-MS data analysis for metabolomics

According to the user guide, process the raw data collected from DDA-MS on MS-DIAL software (Tsugawa et al 2015). In short, use the Reifycs ABF converter (http://www.reifycs.com/AbfConverter/index.html) to convert the raw MS data from the supplier's file

format (.wiff) to the universal file format (.abf) in Reifycs Inc.. After conversion, use MS-DIAL software for feature detection, spectral deconvolution, metabolite identification, and peak alignment between samples. Obtain the MS/MS spectra from the MassBank database provided by MS-DIAL software and perform MS/MS-based metabolite identification in MS-DIAL using the obtained MS/MS spectra. The MS 1 and MS/MS information containing metabolites are included in MS-DIAL. Perform lipid identification based on MS/MS spectra by searching the obtained MS/MS spectra in MS-DIAL. The internal computer of the software simulates the MS spectrum database for MS/MS spectra (version number: LipidDBs-VS 23-FiehnO), which includes MS 1 and MS/MS information for common lipid types. The tolerance settings for MS 1 and MS/MS searches are set to 0.01 Da and 0.05 Da, and other parameters used in MS-DIAL are set to their default values.

PRM-MS data analysis

According to the plan (https://www.example.com project/home/software/ Skyline/start. View), process the raw data on Skyline software. Import the original MS data file into the software for peak extraction. Pre-select an adsorbent-product ion pair (transition) for each target lipid, and calculate the peak area corresponding to each transition using the software. Finally, export the results containing lipid identification and quantification in tabular form for further statistical analysis.

Proteomics sample preparation

A total of 47 AD patients and 35 healthy controls were used for proteomics studies. According to the manufacturer's recommendations, plasma (4 μL crude plasma) was subjected to multiple affinity removal system (MARS) Human-14 column (Agilent) to remove high-abundance proteins. The fractions were collected (low-abundance proteins), then digested according to the manufacturer's Filter Assisted Sample Preparation (FASP) protocol. Proteins were digested overnight in 50 mM NH 4 HCO 3 buffer at a protein-to-enzyme ratio of 50:1 with trypsin at 37 °C, and the released peptides were collected by centrifugation and evaporated under vacuum.

LC-MS analysis for proteomics

The sample (1 μg) was analyzed on a self-made C18 column (75 μm × 15 cm, 3 μm). The U3000 ultra-high-performance liquid chromatography system is connected to the Q-Exactive HF mass spectrometer (Thermo Scientific). Peptides were separated by linear gradient elution from 5% to 35% ACN containing 0.1% formic acid over 60 minutes at a flow rate of 300 nL/min, and then increased linearly to 80% ACN within 1 minute. Increased linearly to 80% ACN within 1 minute and maintained for 3 minutes. The column was rebalanced in 5% acetonitrile for 5 minutes. Rebalanced for 5 minutes. The operating voltage of the chromatographic source is 2.1 kV. The DDA scheme includes full MS scans with a resolution of 60,000 FWHM (at m/z 200), set to AGC 5E6 (maximum injection time 20 ms). Set to AGC 5E6 (maximum injection time 20 milliseconds), followed by 20 MS/MS scans with a resolution of 15,000 FWHM, set to AGC 5E6 (maximum injection time 20 milliseconds). Then perform 20 MS/MS scans with a resolution of 15,000 FWHM, AGC set to 2E5 (maximum injection time of 100 milliseconds).

Select the 20 most intense precursors, with a separation width of m/z 2 for high-energy collision dissociation (HCD) fragmentation, followed by 27 HCD fragmentation. Set dynamic exclusion to 30 seconds. Obtain the profile type. (For details, see supplementary information). Data analysis is performed using MaxQuant software version 1.6.2.0. (http://www.maxquant.org/) for data analysis. To identify proteins, MS/MS data is submitted to the UniProt Human Proteome Database (3.43 version, 72,340 sequences). The Andromeda search engine is used to submit to the UniProt Human Proteome Database (3.43 version, 72,340 sequences), with the following settings: trypsin digestion; fixed modifications: cysteine methylation; variable modifications: methionine oxidation; maximum modification: cysteine methylation. Variable modification for methionine oxidation; up to two missed cleavages; false discovery rate calculated from the search bait database. Other parameters are set to default values. Unlabeled quantification (LFQ) was also performed in MaxQuant. The minimum ratio count for LFQ is set to 2, and the run-to-run matching option is set to 1 minute. Other parameters are set to their default values. Other parameters are set to their default values.

Statistical analysis

Statistical analysis was performed using SPSS 26.0 software. All results were analyzed using ANOVA or Student's t-test, with mean ± standard error notation. A $p < 0.05$ was considered statistically significant. UPLC-Q-TOF/MS technology was used to collect spectral information, and peak identification, peak matching, retention time (RT), and mass (M/Z) data from XCMS and VGDB were compared. Three-dimensional data information was imported into R software.

Principal Component Analysis (PCA) and Partial Least Squares Discriminant Analysis (PCA-da) were used to obtain clustering information and important variables. PLS-DA model was employed to calculate VIP values for each variable in the sample. Metabolites with VIP > 1.05 were selected as differentially expressed metabolites at various time points across groups.

Data was normalized and transformed logarithmically, and t-tests were used to calculate P values. When there was no biological replication, only fold changes were calculated. Metabolites with log2-fold change ≥1 and P ≤ 0:05 were selected as the final differentially expressed metabolites. Qualitative analysis of primary and secondary spectra data from mass spectrometry was conducted based on Very Genome Database (VGDB), and substance analysis was performed by referencing other public mass spectrometry databases such as MassBank, METLIN, HMDB, and MONA. Finally, the metabolic pathway analysis was performed using MetaboAnalyst 5.0 (https://www.metaboanalyst.ca/).

RESULTS

Overview of research workflow

Blood plasma samples were collected from 47 AD patients and 35 control plasma samples from the general population. The age, gender, and MMSE scores of AD patients compared with the normal control group are shown in Table S1.Non-targeted metabolomics, lipidomics, and proteomics studies based on

LC-MS were conducted to identify biomolecules that may be dysregulated in AD patient plasma. Statistical analysis and data mining revealed abnormal expression of certain metabolites, lipids, and proteins in AD patients. Bioinformatics analysis elucidated the abnormal expression of these metabolites, and targeted quantitative analysis using LC-MS (PRM) was employed to validate some of the omics results. Finally, ROC curves for dysregulated molecules were calculated, along with their correlation with clinical factors in AD, to evaluate their potential use as biomarkers for AD diagnosis or prognosis (Figure 1).

Metabolomics analysis and dysregulated metabolites in AD

After processing the raw MS data, principal component analysis (PCA) was used to create an overview of the metabolomics expression profiles of all samples in both positive ion (Figure 2A) and negative ion (Figure 2B) modes. On the PCA score plot, the AD group and the control group show a partial separation trend. Further statistical analysis revealed a total of 31 dysregulated metabolites (23 in positive ion mode (Figure 2C); 8 in negative ion mode (Figure 2D) (FC> 2 and t-test p value <0.05). Additionally, MetaboAnalyst was used to analyze metabolic pathways with significant differences between the AD group and the HC group.

Lipidomics analysis and lipid dysregulation in AD

For the data processing procedures for metabolomics features, PCA is used to summarize the expression patterns of lipids in all samples. Similarly, the results of metabolomics features, both the AD group and the control group show significant separation trends in positive ion mode (Figure 3A) and negative ion mode (Figure 3B). Through MS/MS spectrum comparison, statistical analysis reveals that many lipid characteristics are dysregulated (FC> 2 and t-test p values <0.05) in both the AD group and the control group, particularly in positive ion mode (Figure 3C) and negative ion mode (Figure 3D).

Changes in the Proteomics network in AD

Metabolic pathway enrichment analysis revealed several significantly altered pathways include lysine degradation, pyruvate metabolism, glycine, serine, and threonine metabolism, linolenic acid metabolism, and arginine and proline metabolism(Figure 4). Separately, PCA showed a trend of separation between the AD and control groups (Figure 2).

Changes in the Lipidomics network in AD

Some dysregulated lipids are upregulated in the AD group, such as Cer 40:9;O3, DG 46:7, TG 45:7, PC O-35:5, DG 25:0, NAE 18:4, NAE 16:1, NAE 16:2, and ST 28:1;O; while some are downregulated, such as DG 44:11, SM 32:7;O3, PC O-33:6, SM 35:7;O3, DG 25:4, DG 26:4, DG 23:4, DG 27:4, DG 24:4, DG 37:7, CAR 18:2, SM 41:1;O2, SM 40:0;O3, SM 40:2;O2, DG O-37:1, and SM 34:2;O3. (Figure 5).

Using the LINEX software, lipidomics networks that connect lipid substances are provided, as shown in Figures 6A, 6B. It showed a global view of lipidome changes between the control group and the case

group. In these networks, each node represents a type of lipid, and each edge between pairs of lipids indicates biochemical reactions that convert one lipid substance into another within or between categories. The color of the edges represents the type of reaction (i.e., FA removal, FA addition, HG removal, HG addition), and the size of the nodes indicates the significance of differences between AD and normal control groups (the larger the node, the more pronounced the change in lipid). In Figure 6A, node colors indicate log-fold changes between the two conditions (red: higher levels in AD patients, blue: lower levels in AD patients), while in Figure 6B, node colors represent lipid categories. Regarding the type of reaction, HG removal is the most common type (highlighted in green in Figure 6B), indicating that pathways involving this type of metabolic reaction are particularly affected by AD. The Figure 6C showed the enrichment network generated by LINEX based on the global network. The algorithm highlights a subnetwork that maximizes reaction differences between the control and case conditions. The resulting subnetwork consists only of PC and LPC lipid substances and reactions from LPC to PC, which can be catalyzed by phospholipases (such as RHEA: 36231, RHEA: 44068, RHEA: 40579).

Validation of candidate biomarkers and analysis of AD correlation

Targeted lipid quantification based on PRM was performed to quantify 32 lipids. As shown in Figure 7, seven lipids were significantly upregulated in the AD group, Cer 40:9;O3, DG 25:0, DG 46:7, NAE 16:1, PC(20:1/22:5), PC O-35:5, and TG 45:7. Further ROC curve analysis revealed that the AUCs for these seven lipids were greater than 0.8,with Cer 40:9;O3 (AUC 0.884, 95% CI 0.732-0.913),DG 25:0 (AUC 0.824, 95% CI 0.715-0.911),DG 46:7 (AUC 0.884, 95% CI 0.809-0.947),NAE 16:1 (AUC 0.84, 95% CI 0.756-0.916),PC(20:1/22:5) (AUC 0.816, 95% CI 0.724-0.902), PC O-35:5 (AUC 0.877, 95% CI 0.784-0.94),TG 45:7. (AUC 0.833, 95% CI 0.737-0.919).

DISCUSSION

In 2024 the Alzheimer's Association Workgroup revised the diagnostic and staging criteria for AD. The updated framework highlights core 1 biomarkers, including CSF or plasma Aβ42, p-tau217, p-tau181, p-tau231, and amyloid PET, all of which map onto either the amyloid beta pathway or the AD tauopathy pathway(Clifford R, et al., 2011).However, CSF testing is invasive and PET imaging is expensive, we want to search for other plasma biomarkers, such as metabolomics markers.In this study, 82 participants were recruited. The blood samples were quantified by the LC–MS/MS and HPLC plus Q-Exactive HF MS. The analyzed results of Proteomics that lysine degradation, pyruvate metabolism, glycine, serine and threonine metabolism, linolenic acid metabolism and arginine and proline metabolism, were changed in the amino acid metabolic pathways. Further, The results of the lipidomics analysis showed that seven lipids, such as Cer 40:9;O3, DG 25:0, DG 46:7, NAE 16:1, PC(20:1/22:5), PC O-35:5, and TG 45:7, were markedly increased in the AD group, associated with AUC values greater than 0.8.

Our multi-omics approach has identified a signature of seven plasma lipids that are significantly dysregulated in AD and exhibit promising diagnostic potential. This finding gains mechanistic relevance when considering the specific biological roles of these lipids. For instance, the elevated level of Cer

40:9;O3 aligns with the established link between ceramides and AD pathogenesis. Cer 40:9;O3 (Ceramide) is closely related to AD for potentially linked to Aβ.Ceramides are known to directly influence the activity of β- and γ-secretases, the enzymes responsible for generating Aβ from APP. Elevated very-long-chain ceramides (like C40) can promote a lipid raft environment that facilitates the colocalization of these secretases with APP, thereby increasing amyloidogenic processing.Ceramides are potent pro-apoptotic and pro-inflammatory signaling molecules. They can activate astrocytes and microglia (the brain's immune cells), driving the production of pro-inflammatory cytokines like TNF-α and IL-1β. This chronic neuroinflammation creates a toxic environment that accelerates neuronal damage and synergizes with Aβ pathology (Kalkman,et al.,2025).Our observation of elevated plasma ceramide levels in Alzheimer's disease patients further supports its potential value in AD diagnosis.Recent studies have confirmed that long-chain ceramides, such as Cer 40:9;O3, show a significant positive correlation with plasma p-tau217 levels (Rho = 0.723–0.753), suggesting that they may amplify tau pathology by activating neuroinflammation (microglia/astrocytes) (James D Doecke et al.,2025;Sylvain Lehmann et al.,2025).

Similarly, the increase in TG 45:7 may predict the application prospects of clinical diagnosis of AD.TG 45:7 (Triacylglycerol) is potentially Linked to Energy Metabolism & Oxidative Stress: The high number of double bonds makes this triglyceride and its constituent fatty acids highly susceptible to lipid peroxidation. This peroxidation generates reactive aldehydes like 4-hydroxynonenal (4-HNE), which are profoundly toxic. 4-HNE can adduct to and impair key proteins involved in neuronal energy metabolism (e.g., glucose transporters, mitochondrial enzymes), synaptic function, and Aβ clearance, exacerbating metabolic deficits in the AD brain (Sue,et al.,2016;Qing Gao,et al.,2025).

A decrease in the ether phospholipid PC O-35:5 disrupts cell membrane integrity, increasing the likelihood of contact between β-secretase and APP. A 2025 lipidomics study revealed a negative correlation between PC-type lipids and plasma p-tau181 levels ($r = -0.38$, $p < 0.01$), potentially attributable to reduced membrane fluidity rendering tau protein more susceptible to phosphorylation by kinases. Integrating phospholipid profiling with p-tau181 measurement improved the diagnostic AUC for Alzheimer's disease to 0.88 (specificity: 82%), outperforming individual biomarkers (Lourdes Álvarez-Sánchez,etal.,2025).

There is no direct mention of a specific association between the lipid PC(20:1/22:5), DG 25:0, DG 46:7, NAE 16:1 and Alzheimer's disease (AD) in the provided literature.Our research has clarified the relationship between the lipid and AD.Thare are some potential Mechanisms Linking Phospholipids to Alzheimer's Disease.Phospholipids, including various forms of phosphatidylcholine (PC), are fundamental building blocks of cell membranes in the brain. The composition of these lipids can influence membrane fluidity, integrity, and the function of proteins embedded within them, such as those involved in generating amyloid-beta peptides .

Changes in specific phospholipids could affect the structure of cell membranes. This might alter the interaction between the amyloid precursor protein (APP) and the secretase enzymes that process it.

Depending on the nature of the change, this could potentially facilitate the production of amyloid-beta, a key pathological protein in AD .Phospholipids containing polyunsaturated fatty acids (PUFAs), like the 22:5 fatty acid in PC(20:1/22:5), are particularly susceptible to damage by oxidative stress, which is a known factor in AD progression.Lipids are active signaling molecules. Alterations in phospholipid profiles can drive neuroinflammatory processes, which are a central feature of AD pathology. Inflammatory cells in the brain, like microglia, can be activated by damaged lipids or shifts in lipid balance [Arnsten et al.,2025].

Widespread lipid metabolism disorder is a recognized core feature in Alzheimer's disease [Harald Hampel,et al.,2021].Abnormal lipid environment may promote the production and aggregation of β-amyloid protein (Aβ), as well as exacerbate the excessive phosphorylation of tau protein [Ferreira Silva et al.,2019].

When these seven lipids are combined with the p-tau217/Aβ42 ratio, they may significantly reduce the "gray zone" (proportion of indeterminate results). For instance, a dual-cutoff strategy for p-tau217/Aβ42 has already decreased the intermediate zone from 16% to 8%, and incorporating the lipid profile could further optimize this (Sylvain Lehmann et al.,2025). Studies indicate that the combination of p-tau217, Aβ42/40, and lipid biomarkers achieves an AUC of 0.957 in preclinical Alzheimer's disease, approaching the accuracy of PET imaging (James D Doecke et al.,2025),a prospect our findings strongly support.

LIMITATIONS

This study has several limitations. First, its single-center, cross-sectional design limits the generalizability of the findings and prevents the assessment of how these lipid biomarkers change throughout the different stages of AD. Future longitudinal, multi-center studies are required to validate our findings and observe the dynamics of these lipid biomarkers. Second, the cognitive assessment relied primarily on the MMSE; incorporating more comprehensive batteries like ADAS-cog or MoCA could provide a deeper understanding. Finally, variations in pre-analytical sample handling and the use of different analytical platforms across laboratories pose challenges for the standardization and widespread adoption of these biomarkers.

CONCLUSION

In conclusion, our integrated lipidomics and proteomics analysis has identified a panel of seven plasma lipids that are consistently dysregulated in AD and hold significant value as diagnostic biomarkers. These findings not only underscore the role of specific metabolic pathways in AD pathophysiology but also demonstrate the potential of plasma-based lipid profiling as a practical and informative tool for AD diagnosis. Future efforts should focus on the longitudinal validation of these biomarkers in larger, diverse cohorts to fully establish their clinical utility for disease monitoring and early detection.

Abbreviations

AA
arachidonic acid
Ach
acetylcholine
Ac-PUT
N1-acetyl-putrescine
Ac-SPM
N1-acetylspermine
AD
Alzheimer’s disease
CE-MS
capillary electrophoresis-mass spectrometry
Cers
ceramides
CI
chemical ionization
CL
cardiolipin
CNS
central nervous system
DG
diacylglycerol
dAMP
deoxyadenosine monophosphate
DCA
deoxycholic acid
DHA
docosahexaenoic acid
DI-MS
direct infusion mass spectrometry
EI
electron ionization
GCMS
gas chromatography-mass spectrometry
GDCA
glycodeoxycholic acid
GLCA
glycolithocholic acid
GlcNAc
N-Acetyl-D-glucosamine

GPC
glycerophosphocholine
GPs
glycerophospholipids
HCD
high-energy collision dissociation
HILIC
hydrophilic interaction liquid chromatography
HPLC-MS
high-performance LC-MS
KEGG
Kyoto Encyclopedia of Genes and Genomes
LC-MS
liquid chromatography-mass spectrometry
LPAs
Lysophosphatidic acids
LysoPC or LPC
lysophosphatidylcholine
LysoPE or LPE
lysophosphatidylethanolamine
MG
monoacylglycerol
MCI
mild cognitive impairment
MUFAs
monounsaturated fatty acids
NAD
nicotinamide adenine dinucleotide
NMR
nuclear magnetic resonance
PA
phosphatidic acid
PC
phosphatidylcholine
PCae
acyl-alkyl phosphatidylcholines
PE
phosphatidylethanolamines
PG
phosphatidylglycerol

PI
phosphatidylinositol
PLA2
phospholipase A2
PLs
phospholipids
PS
phosphatidylserine
PS1 and PS2
presenilin 1 and 2
pTau
hyperphosphorylated tau
RP
reversedphase
S1P
sphingosine 1-phosphates
SAH
S-adenosyl-homocysteine
SDMA
symmetric dimethylarginine
SFAs
saturated fatty acids
SM
sphingomyelin
TG
triacylglycerol
TCA cycle
citrate cycle
TLCA
taurolithocholic acid
TQ-MS
triple quadrupole-mass spectrometry
tTau
total tau
UHPLC or UPLC
ultra-HPLC
UPLC-MS
ultraperformance liquid chromatography-mass spectrometry
WGCNA
weighted correlation network analysis.

Declarations

Acknowledgements

The authors would like to thank all the participants and their guardians for their cooperation and contribution to the development of this protocol. We gratefully acknowledge Prof. Zhiqian Tong (Capital Medical University, Beijing, China) for editing this manuscript and giving suggestions on our study design.

Contributors

Conceptualization, S.Z.Z. and Y.X.Y.; experiments, T.W., X.L.H. and Y.Y.Y.; data analysis and presentation, L.X.L., L.M. and L.Z.; statistical analyses, T.W. and F.M.; writing—original draft, review and editing, T.Y.Z., Z.H.S. and H.Y.W. All authors have read and agreed to the published version of the manuscript.

Funding

This study was supported by the National Natural Science Foundation of China (grant no. 62177004).

Competing interests

None declared.

Patient consent

Informed consent was obtained from all subjects involved in the study. The blood collection process followed strict scientific protocols to ensure compliance with EU-GDPR and relevant data protection regulations. This guaranteed that all personal and health data were treated anonymously, securely and confidentially. No individual information was provided to the research team for subsequent demographic analysis.

Ethics approval

Ethics approval was obtained from the Medical Ethics Committee of the Beijing Geriatric Hospital (approval number: BJLLYY-2024-009).

Provenance and peer review

Not commissioned; externally peer reviewed.

Clinical trial number

not applicable

Data availability

The datasets used and/or analysed during the current study available from the corresponding author on reasonable request.

Consent to Participate declaration

Every human participant provide their consent

References

2019. Global, regional, and national burden of Alzheimer's disease and other dementias, 1990-2016: a systematic analysis for the Global Burden of Disease Study 2016. *Lancet Neurol,* 18**,** 88-106.

Amy F T Arnsten, Kelly Del Tredici, Nicolas R Barthélemy,et al., 2025.An integrated view of the relationships between amyloid, tau, and inflammatory pathophysiology in Alzheimer's disease.Alzheimers Dement.doi: 10.1002/alz.70404.

Cravatt, B. F., Simon, G. M., and Yates, J. R., 3rd.2007. The biological impact of mass-spectrometry-based proteomics. *Nature,* 450**,** 991-1000.

Clifford R. Jack Jr, et al. 2024.Revised criteria for diagnosis and staging of Alzheimer’s disease: Alzheimer's Association Workgroup.Alzheimer dementia.DOI: 10.1002/alz.13859.

Food and Drug Administration. FDA clears ffrst blood test used in diagnosing

Alzheimer’s disease. Silver Spring, MD: Food and Drug Administration (2025).

Jack Jr CR, Albert MS, Knopman DS, McKhann GM, Sperling RA, Carrillo MC, et al. 2011.Introduction to the recommendations from the National Institute on Aging-Alzheimer’s Association workgroups on diagnostic guidelines for Alzheimer’s disease. Alzheimers Dement.7(3):257-62.

James D Doecke, Ahmed Chenna , Mintzu Lo,et al., 2025.Combining Lumipulse p-tau217 and Aβ42/40 as confirmatory tests for Aβ positivity prior to disease-modifying therapy.Alzheimers Dement.doi: 10.1002/alz.70707.

Hans O Kalkman, Lukasz Smigielski.2025. Ceramides may Play a Central Role in the Pathogenesis of Alzheimer's Disease: a Review of Evidence and Horizons for Discovery.Mol Neurobiol. doi: 10.1007/s12035-025-04989-0.

Harald Hampel, Robert Nisticò, Nicholas T Seyfried, et al.,2021.Omics sciences for systems biology in Alzheimer's disease: State-of-the-art of the evidence.Ageing Res Rev.doi: 10.1016/j.arr.2021.101346. Epub 2021 Apr 27.

KARRAN, E., MERCKEN, M. & DE STROOPER, B. 2011. The amyloid cascade hypothesis for Alzheimer's disease: an appraisal for the development of therapeutics. Nat Rev Drug Discov, 10**,** 698-712.

Livingston, G., Sommerlad, A., Orgeta, V., Costafreda, S. G., Huntley, J., Ames, D., Ballard, C., Banerjee, S., Burns, A., Cohen-Mansfield, J., Cooper, C., Fox, N., Gitlin, L. N., Howard, R., Kales, H. C., Larson, E. B., Ritchie, K., Rockwood, K., Sampson, E. L., Samus, Q., Schneider, L. S., Selbæk, G., Teri, L., and Mukadam, N.2017. Dementia prevention, intervention, and care. *Lancet,* 390**,** 2673-2734.

Lourdes Álvarez-Sánchez,Laura Ferré-González,Carmen Peña-Bautista,et al.,2025.New approach to specific Alzheimer's disease diagnosis based on plasma biomarkers in a cognitive disorder cohort.10.1111/eci.70034.

Sun, L., Jia, Y., Shi, M., Yang, P., Wang, Y., Liu, F., Chen, G.-C., Zhang, Y., and Zhu, Z.2022. Association between Human Blood Metabolome and the Risk of Alzheimer's Disease. *Ann Neurol.,* 95**,** 756-767.

Mahajan, U. V., Varma, V. R., Griswold, M. E., Blackshear, C. T., An, Y., Oommen, A. M., Varma, S., Troncoso, J. C., Pletnikova, O., O'Brien, R., Hohman, T. J., Legido-Quigley, C., and Thambisetty, M.2020. Dysregulation of multiple metabolic networks related to brain transmethylation and polyamine pathways in Alzheimer disease: A targeted metabolomic and transcriptomic study. *PLoS Med,* 17**,** e1003012.

Marcos Vinícius Ferreira Silva, Cristina de Mello Gomide Loures, Luan Carlos Vieira Alves, Leonardo Cruz de Souza, Karina Braga Gomes Borges, Maria das Graças Carvalho.2019.Alzheimer's disease: risk factors and potentially protective measures.J Biomed Sci. doi: 10.1186/s12929-019-0524-y.

Ong,S.E. Mann,M. 2005. Mass spectrometry-based proteomics turns quantitative. *Nat Chem Biol,* 1**,** 252-62.

Qing Gao, Linlin Jiang, Yuting Sun,et al., 2025.Oxidative stress: from molecular studies to clinical intervention strategies.Frontiers in Molecular Biosciences.04 September. DOI 10.3389/fmolb.2025.1638042.

Saito, K., and Matsuda, F. 2010. Metabolomics for functional genomics, systems biology, and biotechnology. *Annu Rev Plant Biol,* 61**,** 463-89.

Shi, J., Sabbagh, M. N., and Vellas, B.2020. Alzheimer's disease beyond amyloid: strategies for future therapeutic interventions. Bmj, 371**,** m3684.

Sue H. Lee, Emily Pierce, Manel Ben Aissa,et al., 2016.Chemoproteomic Approach to Characterizing the Role of 4-HNE in Accelerated Cognitive Impairment.Alzheimer's & Dementia.Volume 12, Issue 7S_Part_21.

Sylvain Lehmann, Audrey Gabelle, Marie Duchiron et al., 2025.Comparative performance of plasma pTau181/Aβ42, pTau217/Aβ42 ratios, and individual measurements in detecting brain amyloidosis.EBioMedicine.doi: 10.1016/j.ebiom.2025.105805.

Verberk, I. M. W., Slot, R. E., Verfaillie, S. C. J., Heijst, H., Prins, N. D., van Berckel, B. N. M., Scheltens, P., Teunissen, C. E., & van der Flier, W. M.2018. Plasma Amyloid as Prescreener for the Earliest Alzheimer

Pathological Changes. Ann Neurol, 84, 648-658.

WISHART, D. S. 2016. Emerging applications of metabolomics in drug discovery and precision medicine. *Nat Rev Drug Discov,* 15, 473-84.

Figures

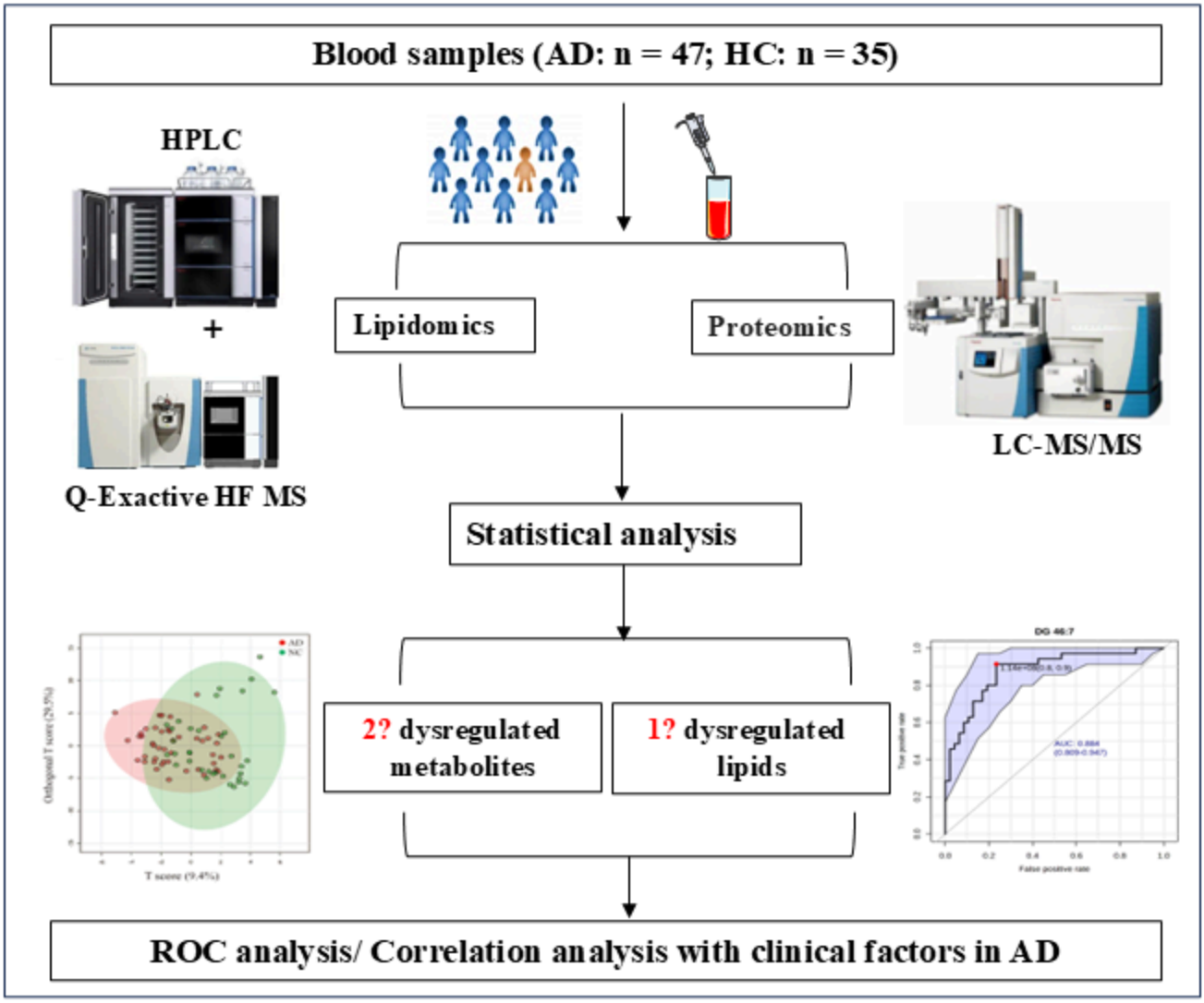


Figure 1

Flowchart of the study workflow. Eighty participates were included in the study, of which 47 were AD patients, 35 heathy volunteers were included as a control group. In the discovery stage, untargeted lipidomics and proteomics were performed to investigate dysregulated molecules in the blood. Pathway enrichment, correlation analysis and ROC analysis were performed to further gain insights from the omics data.

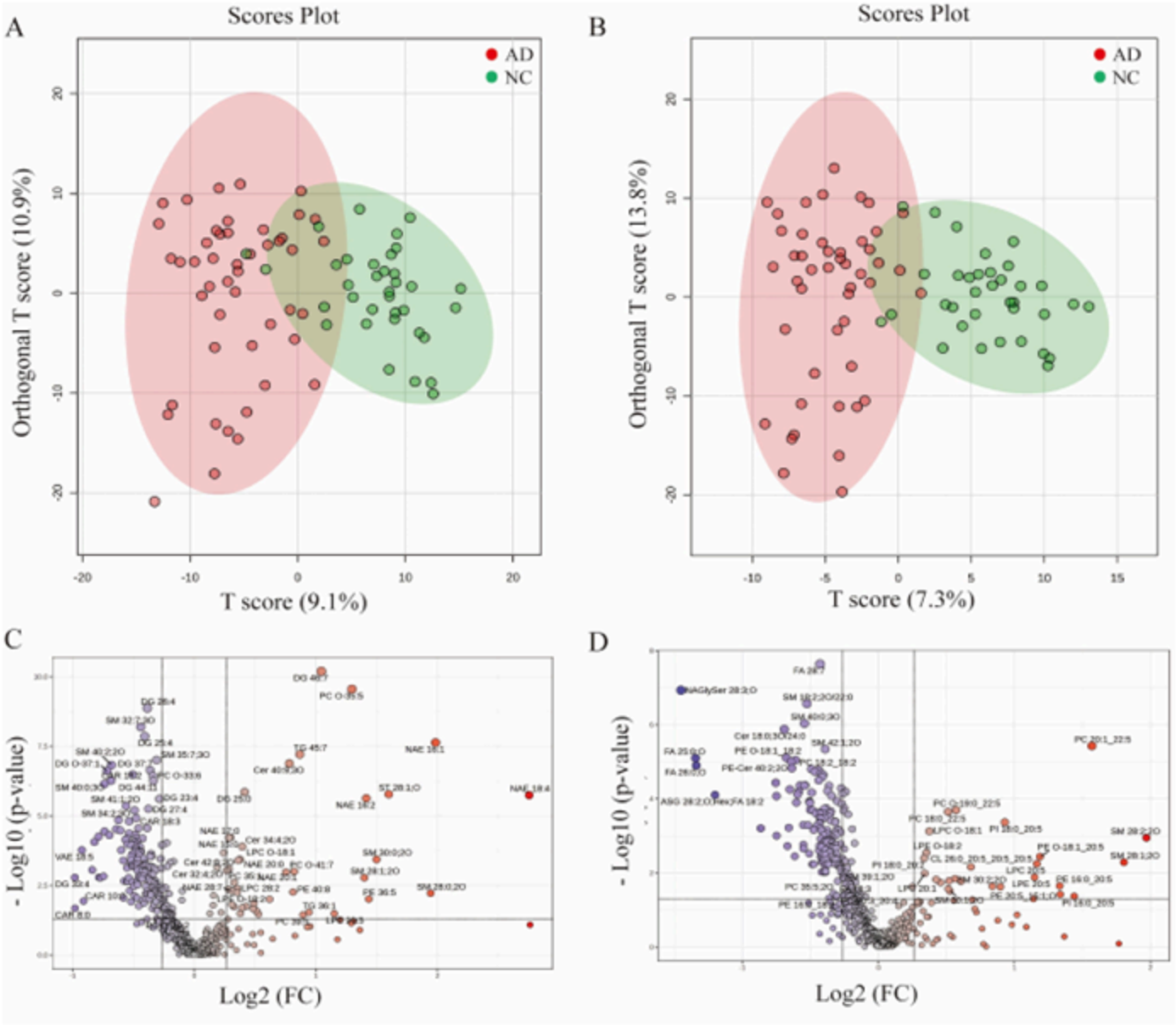


Figure 2

Overview of the untargeted metabolomic results. A Orthogonal PLS-DA score plot for the metabolites detected in positive ion mode. The samples in different groups are presented by different colors: red, AD (n = 47); green, normal control (n = 35). Circles represent the 95% confident interval. B Orthogonal PLS-DA score plot for the metabolites detected in negative ion mode. The samples in different groups are presented by different colors: red, AD (n = 47); green, normal control (n = 35). Circles represent the 95% confident interval. C Scatter plots presenting fold change (FC) and t-test p-value of the identified metabolites in positive ion mode. The X-axis represents the log2-transformed FC, and the Y-axis represents the log10-transformed p-value. D Scatter plots presenting FC and t-test p-value of the

identified metabolites in negative ion mode. The X-axis represents the log2-transformed FC, and the Y-axis represents the log10-transformed p-value

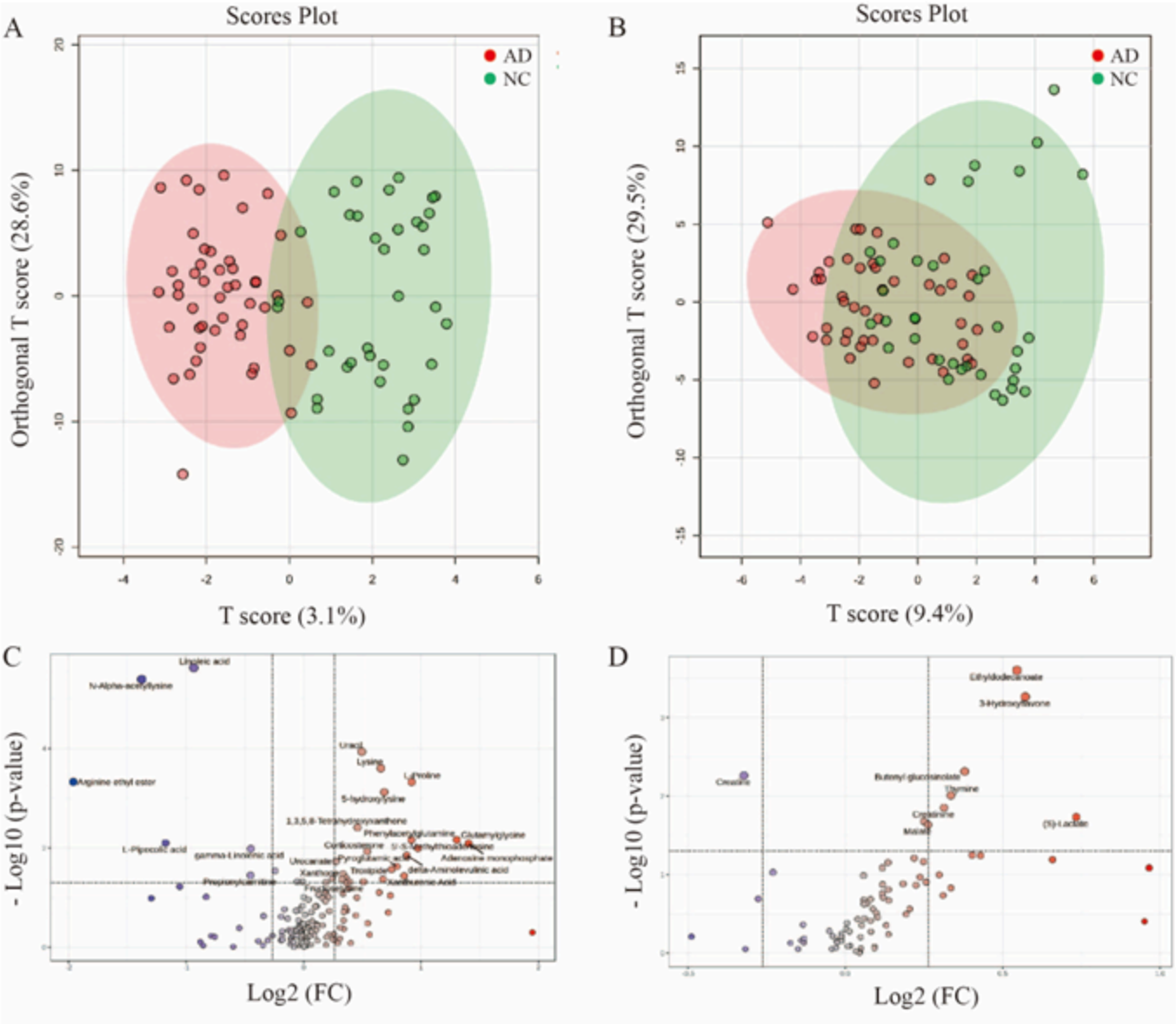


Figure 3

Overview of the untargeted lipidomic results. An Orthogonal PLS-DA score plot for the metabolites detected in positive ion mode. The samples in different groups are presented by different colors: red, AD (n = 47); green, normal control (n = 35). Circles represent the 95% confidence interval. B Orthogonal PLS-DA score plot for the metabolites detected in negative ion mode. The samples in different groups are presented by different colors: red, AD (n = 47); green, normal control (n = 35). Circles represent the 95% confidence interval. C Scatter plots presenting fold change (FC) and t-test p-value of the identified metabolites in positive ion mode. The X-axis represents the log2-transformed FC, and the Y-axis represents the log10-transformed p-value. D Scatter plots presenting FC and t-test p-value of the

identified metabolites in negative ion mode. The X-axis represents the log2-transformed FC, and the Y-axis represents the log10-transformed p-value

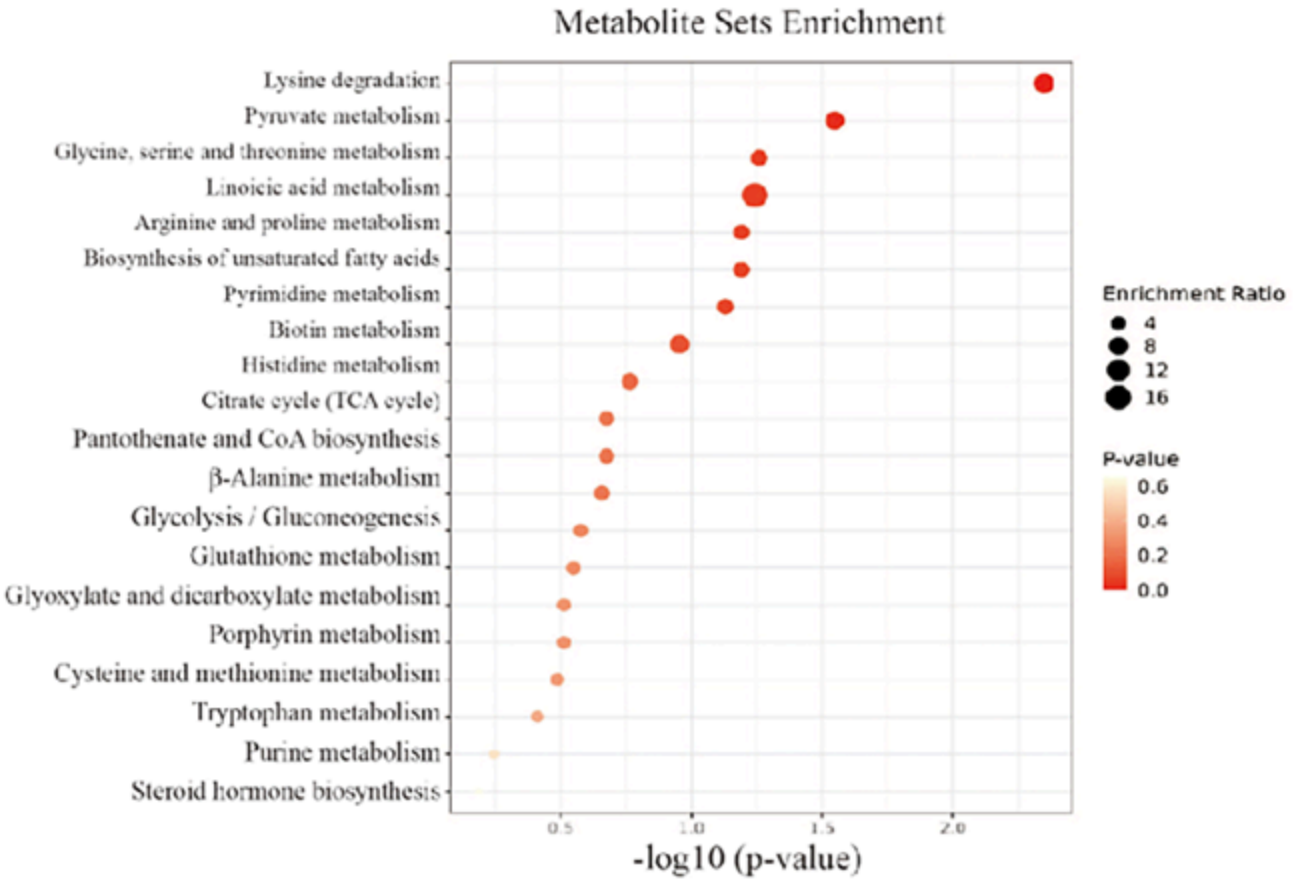


Figure 4

Metabolic pathways enrichment analysis of differential metabolites was conducted based on KEGG database (Bubble chart).

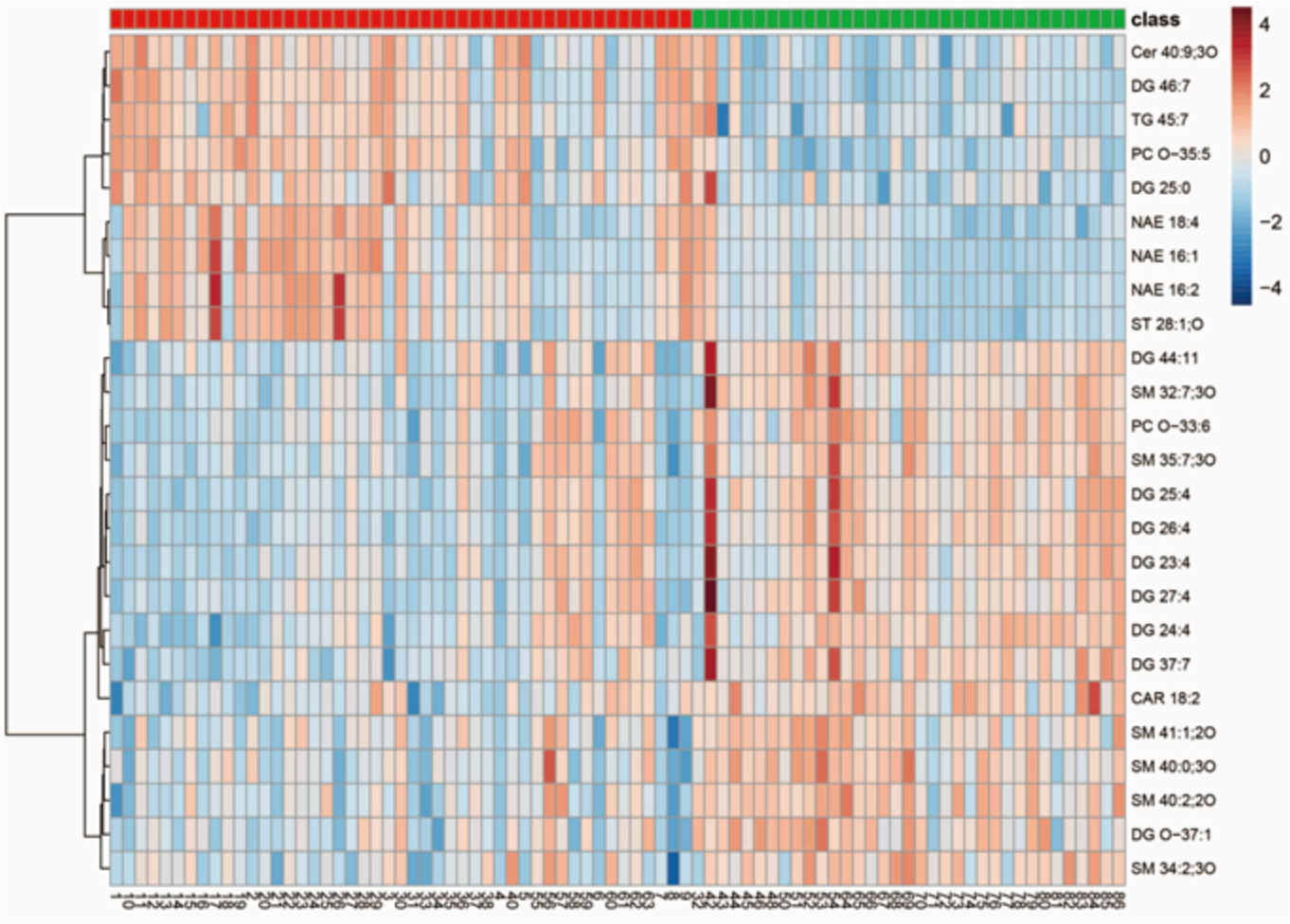


Figure 5

Heat map presenting the expressive patterns of the lipidomic metabolomics in the blood. Sample category is presented in red (AD, n = 47 pooled biological replicates) and green (Heath control, HC, n = 35 pooled biological replicates), and the intensity of protein is presented from blue (low intensity) to red (high intensity).

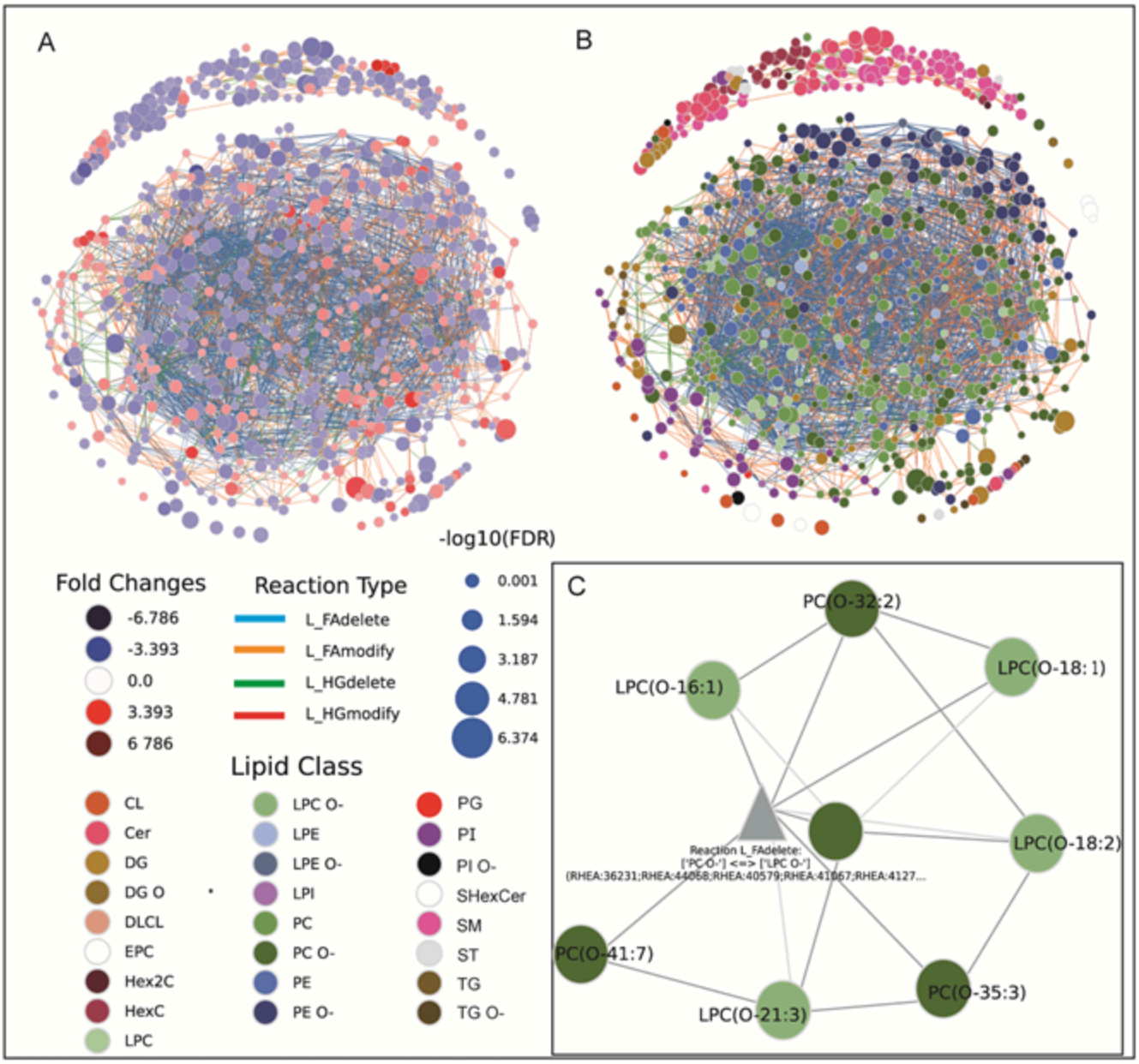


Figure 6

LINEX lipid network based on untargeted lipidomic data. Each node represents a lipid species, and each edge between a pair of nodes indicates a biochemical reaction transforming the lipid species into each other within one class or between classes. Edge colors indicate the reaction types, and node sizes indicate the negative log10 FDR corrected p-values of lipid species between the control and case groups. (A) Node colors represent the log fold change between both groups (red: higher level in the cases and blue: lower level in the cases). (B) Node colors represent the lipid classes. (C) LINEX enrichment network with the PC to LPC reaction at the center. Spherical nodes represent lipids, and the colors refer to LPC (Light green) or PC (dark green) lipid species. Triangular nodes represent the enzyme class.

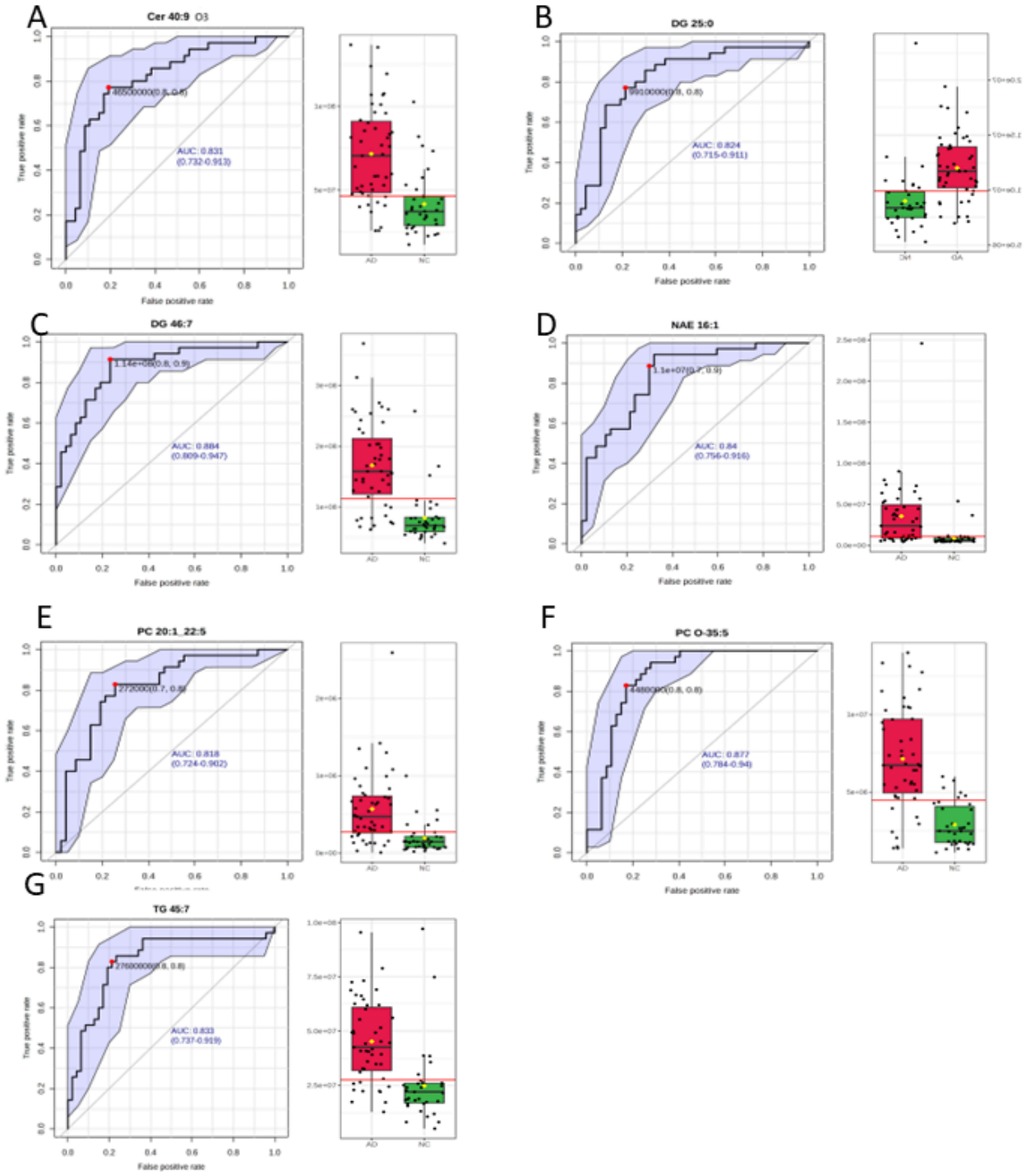


Figure 7

Validation and clinical correlation analysis of the 7 dysregulated lipids. (A-G) ROC curves of lipids (Cer 40:9;O3, DG 25:0, DG 46:7, NAE 16:1, PC(20:1/22-5), PC 0-35:5, PC 0-35:5, TG 45:7 respectively. Red: AD group, n=47; Green: healthy control group, n=35). AUC, 95% confidence intervals, scatter plots, and cutoff values are also shown.

Supplementary Files

This is a list of supplementary files associated with this preprint. Click to download.

- SupplementaryTable1.pptx